HydroCast: Pressure Routing for Underwater Sensor Networks

Youngtae Noh, *Member, IEEE*, Uichin Lee, *Member, IEEE*, Saewoom Lee, *Member, IEEE*,
Paul Wang, Luiz F. M. Vieira, *Member, IEEE*, Jun-Hong Cui, *Member, IEEE*,
Mario Gerla, *Fellow, IEEE*, and Kiseon Kim, *Senior Member, IEEE*

Abstract—A Sensor Equipped Aquatic (SEA) swarm is a sensor *cloud* that drifts with water currents and enables 4-D (space and time) monitoring of local underwater events such as contaminants, marine life, and intruders. The swarm is escorted on the surface by drifting sonobuoys that collect data from the underwater sensors via acoustic modems and report it in real time via radio to a monitoring center. The goal of this study is to design an efficient anycast routing algorithm for reliable underwater sensor event reporting to any surface sonobuoy. Major challenges are the ocean current and limited resources (bandwidth and energy). In this paper, these challenges are addressed, and HydroCast, which is a hydraulic-pressure-based anycast routing protocol that exploits the measured pressure levels to route data to the surface sonobuoys, is proposed. This paper makes the following contributions: a novel opportunistic routing mechanism to select the subset of forwarders that maximizes the greedy progress yet limits cochannel interference and an efficient underwater *dead end* recovery method that outperforms the recently proposed approaches. The proposed routing protocols are validated through extensive simulations.

Index Terms—Anycast, autonomous underwater vehicles (AUVs), opportunistic routing, pressure routing.

I. INTRODUCTION

U NDERWATER sensor networks have been proposed recently to support time-critical aquatic applications such as submarine tracking and harbor monitoring [1], [2]. Unlike

Y. Noh is with the Department of Computer Science and Information Engineering, Inha University, Incheon, 420-751 Korea (e-mail: ytnoh@inha.ac.kr).

U. Lee is with the Department of Knowledge Service Engineering, Korea Advanced Institute of Science and Technology (KAIST), Daejeon 305-701, Korea (e-mail: uclee@kaist.edu).

S. Lee and K. Kim are with the Gwangju Institute of Science and Technology (GIST), Gwangju 500-712, Korea (e-mail: spout2@gist.ac.kr; kskim@gist.ac.kr).

P. Wang is with Morgan Stanley & Co. LLC, New York, NY 10036 USA (e-mail: Paul.Wang@morganstanley.com).

L. F. M. Vieira is with the Departamento de Ciência da Computação, Universidade Federal de Minas Gerais, Belo Horizonte-MG, 31270-901 Brazil (e-mail: lfvieira@dcc.ufmg.br).

J.-H. Cui is with the Computer Science and Engineering Department, University of Connecticut, Storrs, CT 06269-4155 USA (e-mail: jcui@engr.uconn.edu).

M. Gerla is with the Department of Computer Science, University of California at Los Angeles (UCLA), Los Angeles, CA 90095 USA (e-mail: gerla@cs.ucla.edu).
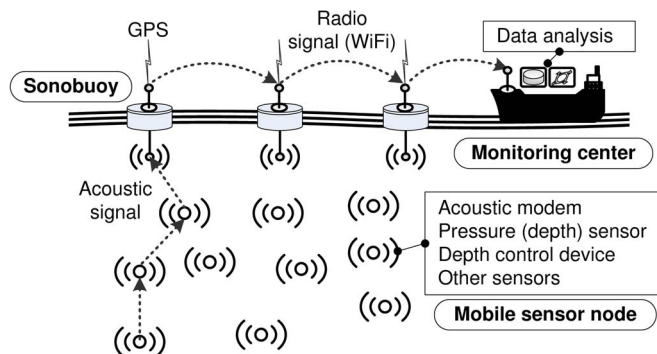
Fig. 1. SEA swarm architecture.

traditional tethered sensors, a large number of underwater mobile sensor nodes are dropped in the venue of interest to form a Sensor Equipped Aquatic (SEA) swarm that moves as a group with the water current [3], [4]. Each sensor is equipped with a low-bandwidth acoustic modem and with various sensors (e.g., Drogues [5]). Moreover, each sensor can control its depth through a fish-like bladder apparatus and a pressure gauge. The swarm is escorted by sonobuoys on the sea surface; the sonobuoys are equipped with acoustic and radio (e.g., WiFi or satellites) communications and GPS (see Fig. 1). There are several significant advantages of the SEA swarm architecture. First, mobile sensors provide 4-D (space and time) monitoring, thus enabling dynamic monitoring coverage. Second, the multitude of sensors in the SEA swarm provides extra control in redundancy and granularity. Third, the floating sensors increase the system reconfigurability because they can control their depth; moreover, they resurface once depleted of energy and can be recovered and reused.

In the SEA swarm architecture, each sensor monitors local underwater activities and reports time-critical data to any available sonobuoy using acoustic multihopping; then, the data are delivered to a monitoring center using radio communication. The primary focus of this paper is to design an efficient anycast routing protocol from a mobile sensor to any sonobuoy at sea level. However, this is challenging due to the node mobility and limited resources (bandwidth and energy) of the mobile sensors. An underwater acoustic channel has a low bandwidth and propagation latency five orders of magnitude higher than the radio channel [6]. Acoustic transmissions consume significantly more energy than terrestrial microwave communications. Therefore, such severe limitations in the communication

bandwidth, coupled with high latency and limited energy, make the network vulnerable to congestion due to packet collisions. Under these circumstances, minimizing the number of packet transmissions is important for two reasons: minimizing congestion and minimizing energy consumption.

The conventional proactive/reactive routing protocols (e.g., OLSR, AODV, etc.) rely on systematic flooding for route discovery and maintenance, which potentially causes excessive energy consumption and collisions. In the SEA swarm scenario, general 3-D geographic routing is preferable because it is stateless. However, geographic routing requires online distributed localization of mobile sensors; it is expensive and requires a long time to converge. Moreover, Durocher *et al.* [7] demonstrated that efficient recovery from a local minimum may not always be feasible in 3-D geographic routing; thus, it requires an expensive exhaustive search including 3-D flooding and random walks [8].

In this paper, the georouting problem is specialized in that it is anycast to any sonobuoy on the surface. Thus, it suffices to route a packet upward to shallower depths. Given that the onboard hydraulic pressure gauge can accurately estimate depth (avg. error < 1 m [9]), the depth information can be used for geographic anycast routing. Yan *et al.* [10] recently proposed a *greedy* method called depth-based routing (DBR) [10] where the packet forwarding decisions are made locally based on the measured pressure level (or depth) at each node so that a packet is greedily forwarded to the node that has the lowest pressure among its neighbors. However, a forwarding node might not locate neighbors with a lower pressure level if it encounters a void region in the swarm. Similar to face routing in the 2-D approaches [11], it must return to the recovery mode to route the packet around the void, but this was not addressed in [10]. Note that this hydraulic-pressure-based anycast routing is stateless and does not require expensive distributed localization [12]. In the proposed scenario, the tagging of the sensed data with its location can be performed when the data come to the surface. For example, a monitoring center can efficiently perform *offline localization* using only the local neighbor information collected from each node.

The key challenges of hydraulic-pressure-based routing are the unreliable acoustic channel and the presence of voids; thus, it requires efficient greedy forwarding and dead-end recovery methods. In this paper, these challenges are addressed, and a generalized hydraulic-pressure-based anycast routing protocol called HydroCast is proposed. The following are the key contributions of this paper.

The wireless channel quality is considered, and simultaneous packet receptions among a node's neighbors are exploited to enable opportunistic forwarding via a subset of the neighbors that have received the packet correctly. To suppress the hidden terminals, the existing forwarding set selections use a heuristic to choose nodes in a geographic region facing the direction toward the destination (in this paper, upward) [10], [13]–[15]. It is demonstrated that these approaches do not maximize the expected progress toward the destination, and in general, locating such a set is computationally difficult. Thus, a simple greedy heuristic is proposed that searches for a cluster of nodes with the maximum progress and limited hidden terminals, using the

local topology information only. The simulation results validate that the proposed approach can locate a set whose expected progress is very close to that of the optimal solution.

Then, an efficient recovery method with a delivery guarantee is proposed. The key idea is that a node can determine whether it is on the local minimum because only the depth information is used for routing, i.e., a local minimum occurs when neighboring nodes with a lower depth than the current depth do not exist. In the proposed scheme, each local minimum node maintains a recovery route to a node whose depth is lower than itself. After one or more path segments go through the local minima, a packet can be routed out of the void and can switch back to the greedy mode. Because any nodes located beneath the void area can potentially suffer from the void and opportunistic forwarding along the recovery path is feasible, the proposed approach is more efficient than a random-walk-based approach [8]. For efficient route discovery, a route discovery method that implements hop-limited 2-D flooding over the surface of void regions is proposed, and this is a significant improvement over the simple 3-D flooding. Furthermore, the proposed protocol is compared with existing solutions in two different underwater mobility models, i.e., an extended 3-D version of the meandering current mobility (MCM) model [16] for passive (grouped) and relatively slow mobility and the well-known autonomous underwater vehicle (AUV) mobility model [17] for an independent and relatively high speed mobility.

II. BACKGROUND AND RELATED WORK

Types of mobile sensors and their constraints (e.g., communication characteristics and energy consumption) are reviewed, and then, the underwater routing protocols are thoroughly examined.

A. Mobile Underwater Networks and Resource Constraints

Mobile Sensor Types: The most common AUV configuration is a torpedo-like vehicle (e.g., REMUS and IVER2) with a streamlined body with a propeller and control surfaces at the stern [18]. These AUVs have a speed range of 1 knot (0.514 m/s) to 15 knots (7.716 m/s), and most vehicles operate at around 3 knots (1.5 m/s). Another configuration is a glider (e.g., Seagliders [19]) that uses small changes in its buoyancy in conjunction with wings to make up-and-down sawtooth-like movements. Although gliders restrict mobility patterns due to their energy limits, they can provide data collection on temporal and spatial scales that would be costly if traditional shipboard methods are used. Unlike AUVs, underwater floats such as UCSD Drogues and ARGO [20] primarily use a buoyancy controller for depth adjustments and move passively along with the water current.

Resource Constraints of Mobile Sensors: Communications in the underwater acoustic channel have two innate characteristics: low bandwidth and large propagation delays. The available bandwidth of the acoustic channel is limited and strongly depends on both range and frequency. As surveyed by Kilfoyle *et al.* [21], the existing systems have highly variable link capacity, and the attainable range and rate product

rarely exceeds 40 km-kb/s. The signal propagation speed in the acoustic channel is 1.5×10^3 m/s, which is five orders of magnitude lower than the radio propagation speed of 3×10^8 m/s in air. This huge propagation delay has a great impact on network protocol design. For the power consumption, a typical pressure sensor gauge consumes 10–100 μW [22], [23]. Note that this level of power consumption is much smaller than that of a typical accelerometer [24]. However, it is important to note that underwater acoustic modems consume significant amounts of energy compared with terrestrial radios; for example, WHOI Micromodem-2 has an active/receive state with a power consumption of 158 mW and a transmission state with a full power consumption up to 48 W [25].

B. Related Work

Underwater Routing Protocols: Pompili *et al.* [26] proposed two types of underwater routing protocols for delay-sensitive and delay-insensitive applications in a 3-D underwater environment. The delay-sensitive routing protocol is based on virtual circuit routing. The primary and backup multihop node-disjoint data paths are calculated using a centralized controller to achieve an optimal delay. The delay-insensitive routing protocol is a distributed geographic solution that minimizes energy consumption via back-to-back packet transmissions and cumulative acknowledgments. Xie *et al.* [27] proposed the vector-based forwarding (VBF) protocol in which packets are forwarded to the nodes that are located within the route of a given width between the source and the destination. This relay selection algorithm avoids energy consumption by reducing the number of packet relays.

Yan *et al.* proposed a greedy anycast routing solution called DBR [10]. In DBR, packet forwarding decisions are made locally and statelessly based on the pressure (or depth) level measured at each node. The packets are geographically forwarded to nodes with lower depths in a greedy fashion. This hydraulic-pressure-based anycast routing protocol benefits from being stateless and does not require expensive distributed localization [28], [29]. DBR exploits the opportunistic broadcast nature by allowing simultaneous packet receptions and performs greedy forwarding via a subset of the neighbors that have correctly received the packet. Ayaz *et al.* proposed a dynamic addressing-based routing protocol called H2-DAB [30], which relies on beacon messages for routing decisions. H2-DAB is composed of two phases: assigning dynamic addresses to floating nodes and data delivery. In the first phase, a dynamic hop ID is allocated to all floating nodes whose initial hop ID is equal to 99. Sinks begin sending beacon messages downward. Each node that receives a hello packet updates its hop ID according to the number of hops to the sink. As a result, nodes closer to the sinks have a smaller hop ID. This protocol does not require a pressure level sensor or location information while handling the node movement through ocean currents.

Casari *et al.* [31] proposed several reliable broadcasting protocols that leverage the ability to use small bands to transmit an alert packet over a long distance. After sending alert signals, the nodes reduce the transmission range and select only certain neighboring nodes to repeat the broadcast, thereby lowering the total number of transmissions required. Similar ideas can also be found in other studies [32], [33]. Xu *et al.* [34] proposed a novel multiple-path FEC approach (M-FEC) based on Hamming coding to improve reliability and energy efficiency. In the M-FEC, a Markovian model formulates the probability and calculates the overall PER for a forwarding decision. Finally, its feedback scheme can further reduce the number of multiple paths and achieve the desirable overall PER in the M-FEC. Casari *et al.* [35] proposed a routing policy that exploits the channel behavior given some key parameters such as the source position and depth, receiver location, and sea bottom profile. Then, the channel behavior information is translated into signal-to-noise ratio (SNR) statistics. The forwarding is determined based on the constraint that the SNR exceeds a threshold with a given probability. The authors reported that the channel-aware heuristic policy consistently outperforms the shortest path policy and performs very close to the optimal one in the scenarios investigated. Although these types of protocols exploit probability model or statistics to achieve a better tradeoff between reliability and efficiency, they have limitations to the fallback mechanism (i.e., route recovery).

Huang *et al.* [36] proposed the linear coded digraph routing (LCDR) to enhance the end-to-end throughput of TCP-based packet flows in underwater mesh networks. In the LCDR, each ingress node performs network coding and forwards packets based on the available bandwidth on the outgoing links. By harnessing the spare bandwidth on each link, it improves the end-to-end throughput of TCP flows. Recently, Noh *et al.* [37] proposed the void-aware pressure routing (VAPR), which is a beacon-based routing protocol. VAPR is composed of two components: enhanced beaconing to build direction trails and opportunistic directional data forwarding (greedy upward/downward forwarding) according to the directional trails. However, VAPR requires beacon propagation in the entire network. Due to the proactive maintenance of paths, this protocol is suitable for an environment with relatively slow mobility. A detailed survey of recent underwater routing protocols has been presented in the survey papers [35], [38].

Geographic Routing Under Channel Fading: In an SEA swarm scenario, due to the prohibitive cost of route discovery and maintenance, general 3-D geographic routing is preferable because it is stateless. In geographic routing, a packet is greedily forwarded to the node closest to the destination to minimize the average hop count. However, due to channel fading, the further the transmission range, the higher the attenuation and the greater the likelihood of packet loss. Researchers have attempted to incorporate the associated cost, e.g., number of transmissions and energy consumption, into geographic routing [26], [39]. For example, Lee *et al.* [39] proposed a generalized link metric called the normalized advance (NADV) where the amount of progress is normalized by its associated cost. However, these protocols have not considered simultaneous packet receptions by a node's neighbors and their ability of opportunistic packet forwarding by scheduling the set of nodes that received the packet correctly based on their distances (or associated costs) to the destination [13], [14], [40], [41].

A key design issue in opportunistic routing is the selection of a subset of neighbors that can make the best progress toward the

destination but that do not have the hidden-terminal problem. That is, when a higher priority node transmits a packet, other low-priority nodes should be able to suppress forwarding to prevent redundant packet transmissions and collisions. Most opportunistic routing protocols (also called anypath routing), such as ExOR [40] and least-cost opportunistic routing [41], that do not use geographic information require a global topology and link quality information (similar to link state routing) to locate a set of forwarding groups toward the destination; thus, they are more suitable for static wireless mesh or sensor networks. In practice, geographic routing can also benefit from opportunistic forwarding as in geographic random forwarding [14], contention-based forwarding [13], and focused beam routing [15], although these are not optimal due to the lack of global knowledge. In the literature, researchers have typically used a geometric shape (e.g., a triangle or cone [13], [15]) that *faces toward the destination* for forwarding set selection to mitigate hidden-terminal problems. The notion of the expected progress of opportunistic forwarding toward the destination (in meters), called expected packet advance (EPA), was recently established by Zeng *et al.* [42]. However, none of the previous work [13]–[15], [42] attempted to locate a forwarding set with the maximum EPA and without the hidden-terminal problem. In this paper, it is demonstrated that locating such a set is a variant of the maximum clique problem, which is computationally difficult, and thus, a simple greedy heuristic method is proposed that well approximates the optimal solution.

Geographic Routing Recovery Mode: The recovery mode in geographic routing can be classified as stateful or stateless. In 2-D networks, face routing [11] is a widely used stateless (memoryless) strategy. The basic concept is to planarize a network graph using a simple local method and to forward a packet along one or possibly a sequence of adjacent faces, thus providing progress toward the destination node. For 3-D networks, it has been demonstrated that there is no *local* memoryless routing algorithm that delivers messages deterministically such as those in 2-D face routing [7]. Based on this observation, Flury *et al.* [8] proposed a randomized geographic routing using, random walks. Nodes in the network are arranged in a virtual 3-D grid coordinate using a localized algorithm where each grid point is a cluster of nodes in close proximity. Then, a random walk is performed on this virtual coordinate.

There are several stateful approaches proposed in the literature [43]–[45]. Greedy distributed spanning tree routing [43] uses a spanning tree where each node has an associated convex hull that contains the locations of all its descendant nodes in the tree. A node exhaustively searches the tree for recovery by traversing the subtrees one by one. Liu *et al.* [44] proposed a backtracking method over a virtual coordinate system where a packet is routed toward one of the anchors (used to build the virtual coordinate system), hoping that it can switch back to the greedy mode on its way. Geo-LANMAR [45] inherits the group motion support of landmark routing (LANMAR) that dynamically elects cluster heads (landmark nodes). It circumvents voids in the network using the topology knowledge of the landmark nodes as in [44]. In this paper, given the unique characteristic of the scenario where any nodes located beneath the void area can potentially suffer from the

void, keeping some state is considered to reduce the recovery overhead (preventing expensive random walks to overcome the same void) and to exploit opportunistic packet forwarding along the recovery paths.

III. PROBLEM STATEMENT

Instead of using the generalized 3-D geographic routing, which requires an expensive distributed localization due to slow convergence speed, a 1-D geographic anycast routing in a single (vertical) direction to the surface of the ocean is proposed using the depth information from a pressure sensor.[1] This routing simplification is justified through the proposed scenario communications being strictly *vertical*, from the sensors to the surface nodes. The need for global distributed localization is relaxed via offline localization at a monitoring center that uses local distance measurements (collected with sensor data). Given this, the fundamental problem boils down to exploiting opportunistic packet receptions under channel fading and developing an efficient recovery mechanism from a local minimum.

A. Forwarding Set Selection

Due to channel fading, the further the distance, the higher the signal attenuation and the greater the likelihood of packet loss. The progress must be normalized using its associated cost, which can be represented using NADV [39]: For a given node, NADV to a neighbor node n that has the packet delivery probability of p_n and the progress to the destination d_n^P (in meters) is given as $d_n^P/1/p_n = d_n^P \times p_n$. NADV can be extended to opportunistic forwarding as well. All neighboring nodes that receive the packet will assess their priority based on how close they are to the destination, i.e., the closer to the destination, the higher the priority. A node will forward the packet when all nodes with higher progress to the destination fail to send it. This can be easily scheduled by setting a backoff timer proportional to the distance to the destination. Because nodes can hear each other, those nodes with lower priorities will listen to the packet (either a data packet or an ACK packet) transmitted by a higher priority node and suppress their transmissions, thus excluding the possibility of collisions and redundant packet transmissions. Assume that source S has a set of k neighboring nodes Γ_k ordered based on their priorities as $n_1 > n_2 > \cdots > n_k$. The EPA is simply the normalized sum of advancements made by this neighboring set [42]. The highest priority contributes $d_{n_1}^P p_{n_1}$ (= NADV) on average. Since the next node can only contribute if the highest node fails, its contribution is $d_{n_2}^P p_{n_2}(1 - p_{n_1})$. In general, the EPA is given as follows:

$$\text{EPA}(\Gamma_k) = \sum_{i=1}^{k} d_{n_i}^P p_{n_i} \prod_{j=0}^{i-1} (1 - p_{n_j}) \qquad (1)$$

---

[1]Note that distributed localization typically requires many iterations, each of which requires a considerable amount of time due to the large propagation delay and limited bandwidth underwater (often exacerbated by node mobility). This is confirmed in the extended version of this paper, and it is demonstrated that the overhead is closely related to the localization accuracy requirement [46].
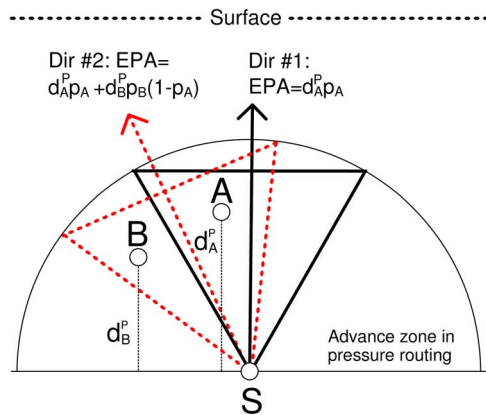
Fig. 2. Impact of direction in pressure routing (Dir #2 > Dir #1).

where $d_{n_i}^P$ denotes the advancement in distance, p_{n_j} denotes the packet delivery probability, and p_{n_0} is defined as 0 for ease of notation.

The given equation demonstrates that as long as a node can make a positive advancement, it can be included to maximize the EPA; however, it is understood that including too many nodes may result in the hidden-terminal problem that leads to redundant transmissions and packet collisions. Because the node degree is higher in 3-D networks than in 2-D networks, 3-D networks have a higher probability of suffering from hidden-terminal collisions than 2-D networks [47]. Despite that minimizing the number of transmissions in resource-constrained sensor networks is one of the most important design criteria, none of the existing solutions [13]–[15], [42] consider the EPA metric and the hidden-terminal problem simultaneously. However, the challenge is that finding such a forwarding set is a variant of the maximal clique problem that determines the largest clique in a graph, which is computationally difficult, rather, to be more precise, finding a clique with maximal EPA. Recall that a clique in a graph is an induced subgraph that is complete (i.e., every node can hear one another). As a simple heuristic, a geometric volume could be used, e.g., a cone with the vertex on the transmitter and the base facing the direction to destination, which is a 3-D extension of 2-D methods reported in [13]–[15]. The problem is that they often fail to maximize the EPA, as shown in Fig. 2. In this paper, simple heuristics are proposed that search for a cluster that maximizes the EPA but limits hidden terminals using only the local topology information. In addition, the proposed approach is validated for locating a set whose EPA is very close to that of the optimal solution.

B. Geographic Routing Recovery Mode

It was reported that for 3-D networks, there is no *local* memoryless routing algorithm that delivers messages deterministically [7]. The state-of-the-art recovery scheme is a randomized geographic routing protocol using random walks [8]. However, this randomized approach may not be suitable for an SEA swarm scenario where nodes need to periodically send their local coordinate information (for offline localization)

and sensor data to the surface nodes. Because nodes vertically forward packets to the surface, any node located beneath the void area can potentially suffer from the void, and every packet originating from that area must perform an expensive random walk to overcome the same void. The overall amortized cost will be very high. It is not yet clear how to exploit the opportunistic packet forwarding using random walks. In addition, O'Rourke *et al.* reported that their prototype system called AquaNode can change depth in water with a speed of 2.4 m/min, spending approximately 0.6 W [48]. However, this topology control is out of scope in this paper as it requires centralized control to reap the benefits of topology control, which cannot be used in our decentralized opportunistic routing protocols.

For these reasons, a stateful approach was adopted as in [43]–[45] and [49]. The key difference from the existing methods was that a node can easily determine whether it is on a local minimum by verifying its neighbors' pressure level. That is, it is on the local minimum if there is no neighboring node with a lower pressure level. If it is assumed that every local minimum node has a recovery route to a node whose depth is lower than itself (either another local minimum or a nonlocal minimum node where greedy forwarding can resume), the scheme successfully recovers from the voids. That is, after one or several path segments go through local minima, the packet can be routed out of the void and can switch back to the greedy mode. Then, the key step is to efficiently locate the recovery routes. The forceful approach is 3-D flooding: i.e., local minimum nodes perform hop-limited 3-D flooding until they locate better escape nodes. In the SEA swarm scenario in this paper, it is noted that the route discovery overhead can be significantly reduced via *route discovery over the void floor surface* using 2-D flooding. However, the challenge is to detect whether a node is on the void floor surface or not. In this paper, an efficient localized void surface floor detection algorithm is presented, and it is demonstrated that the aforementioned local *lower-depth-first* recovery method guarantees packet delivery.

IV. FORWARDING SET SELECTION

A. Packet Delivery Probability Estimation

The following underwater acoustic channel model is used to estimate the delivery probability [6], [50]. The path loss over a distance d for a signal of frequency f due to large-scale fading is given as $A(d, f) = d^k a(f)^d$, where k is the spreading factor, and $a(f)$ is the absorption coefficient. The propagation geometry is described using the spreading factor $(1 \le k \le 2)$; for a practical scenario, k is given as 2. The absorption coefficient $a(f)$ is described using Thorp's formula [50]. Thus, the average SNR over distance d is given as follows:

$$\Gamma(d) = \frac{E_b/A(d, f)}{N_0} = \frac{E_b}{N_0 d^k a(f)^d}. \tag{2}$$

Here, E_b and N_0 are constants that represent the average transmission energy per bit and noise power density in a nonfading additive white Gaussian noise (AWGN) channel. As in [6]

and [51], Rayleigh fading is used to model small-scale fading, where the SNR has the following probability distribution:

$$p_d(X) = \frac{1}{\Gamma(d)} e^{-\frac{X}{\Gamma(d)}}. \tag{3}$$

The probability of error can be evaluated as follows:

$$p_e(d) = \int_0^{\infty} p_e(X) p_d(X) \, dX \tag{4}$$

where $p_e(X)$ is the error probability for an arbitrary modulation at a specific value of SNR X. In this paper, the binary phase-shift keying (BPSK) modulation that is widely used in state-of-the-art acoustic modems is used [52]. In BPSK, each symbol carries a bit. In [53], the probability of bit error over distance d is given as follows:

$$p_e(d) = \frac{1}{2} \left(1 - \sqrt{\frac{\Gamma(d)}{1 + \Gamma(d)}} \right). \tag{5}$$

Thus, for any pair of nodes with a distance d, the delivery probability of a packet with a size of m bits is simply given as follows:

$$p(d, m) = (1 - p_e(d))^m. \tag{6}$$

B. Packet Forwarding Prioritization

A distance-based timer is used to prioritize packet forwarding where the distance denotes the progress toward the surface. When the current forwarder broadcasts a packet, nodes that receive the packet set the timer such that the greater the progress, the shorter the timer. Among those that receive the packet, the highest priority node becomes the next hop forwarder. Then, the remainder of the lower priority nodes suppress their packet transmissions after listening to the next hop forwarder's data or ACK packet.[2]

Unlike [13] and [14], the linear timer function is defined for a receiver x, which is customized for acoustic communications, as $f(d_x^P) = \alpha(R - d_x^P)$, where α is a constant, R is the maximum progress (i.e., transmission range), and d_x^P is the progress of a receiver. Consider two nodes i and j with progress d_i^P and d_j^P, respectively (see Fig. 3). If $d_i^P > d_j^P$, it must be guaranteed that $f(d_i^P) < f(d_j^P)$. Assuming that an ACK is used for suppression, the timer function must satisfy the following inequality: $t_{ci} + f(d_i^P) + t_{ij} + t_{ack} < t_{cj} + f(d_j^P)$, where t_{ab} is the propagation delay from node a to node b, and t_{ack} is the transmission delay of an ACK packet (i.e., hardware receive-to-transmit transition time). Using $f(d^P)$, the following is obtained:

$$\alpha > \frac{t_{ci} - t_{cj} + t_{ij} + t_{ack}}{d_i^P - d_j^P} \tag{7}$$

The numerator is the sum of the propagation delay to travel $d_{ic} - d_{jc} + d_{ij}$ and the ACK transmission delay, as shown in
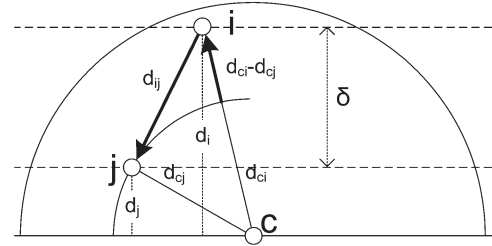
Fig. 3. Timer scheduling for prioritization.

the figure (thick arrows). The progress difference between two nodes $(d_i^P - d_j^P)$ is critical: If it is too small, the constant α will be very large, thus resulting in a very long delay. For a given candidate forwarding set, α can be determined by examining every pair using the local topology information, which requires $O(n^2)$ steps, where n is the number of neighbors. However, α may be too large. To manage this, a system parameter that sets the maximum allowable delay per hop, denoted as γ, exists. In the following, choosing a forwarding set that satisfies the delay constraint is addressed.

C. Forwarding Set Selection Methods

Nodes in the forwarding set must hear each other to mitigate hidden-terminal collisions. Three-dimensional networks have a higher probability of suffering from collisions than 2-D networks because, for equal connectivity, the node degree is higher in 3-D networks than in 2-D networks. At the same time, the progress (i.e., EPA) should be maximized. As discussed earlier, finding the optimal set is computationally difficult, and thus, a simple clustering heuristic is proposed that is inspired by the multipoint distribution relay (MPR) selection in OLSR [54]. To this end, the current forwarder C requires the knowledge of the two-hop connectivity and neighboring nodes' pairwise distances. It is assumed that each node measures the pairwise distance using the time of arrival, which is widely used in underwater networks [12], and the data are periodically reported to the surface for offline localization. This periodic reporting is exploited to obtain the two-hop neighbor information.

It is assumed that node C has computed the NADV of each neighbor as a forwarder *upward* to the surface. As in the MPR selection where a node that covers the highest number of nodes is greedily selected, a simple greedy approach is used here. The greedy clustering begins from the highest NADV neighbor, e.g., S. Node S acquires all other neighbors (of C) at distance $< \beta R$, where β is a constant ($\beta < 1$), and R is the acoustic range. In the proposed design, $\beta = 1/2$ is used so that all nodes clustered by S can hear each other. Then, if other neighbors remain, the clustering proceeds beginning from the highest value remaining neighbor, and so on, until no nodes remain. After this, each cluster is expanded by including all additional nodes such that the distance between any two nodes in the cluster is smaller than R. This condition guarantees that nodes in the set can hear each other. This is repeated for all clusters in turn, and the cluster with the highest EPA is determined. Note that for a given set, the minimum α value for priority scheduling can be found, and this should be smaller than the maximum allowable delay per

hop (γ). Thus, one of the nodes with a lower NADV is removed when detecting $\alpha > \gamma$ during the clustering process.

As an alternative, a *cone shape* (3-D counterpart of a Reuleaux triangle) can be used to select a forwarding set. Unlike the existing approaches [13], [14] that always orient a geometric contention shape along the line between the source and the destination, the forwarding direction that maximizes the EPA must be determined. This requires local topology information—given n neighboring nodes with their depth information and pairwise distances, it is the realization of a graph with n nodes whose edges are weighted based on distance. The local topology is located using the Sweep algorithm that is known to work well for both sparse and dense networks [55]. In Sweep, the process begins from three known vertices, and each neighboring node is localized individually by computing all possible positions consistent with the neighbor positions via a series of bilaterations until all vertices are localized. Using the local topology information, the 3-D space is discretized into a unit degree of θ, thus generating a total of $2\pi^2/\theta^2$ directions over the hemisphere (advance zone). Then, each direction is linearly scanned, and the EPA is calculated to determine the direction with the maximum EPA.

After forwarding the set selection, the chosen forwarding set must be included in the data packet. To reduce the overhead, a Bloom filter, which is a space-efficient membership checking data structure, is used. The membership checking is probabilistic and false positives are possible, but the probability of false positives can be bound by appropriately adjusting the filter size. In a practical scenario, the set size will be smaller than 15 (in the hemisphere advance zone). Fan *et al.* [56] demonstrated that a filter size of 150 bits (19 B) used to represent 15 items has a false positive rate of less than 1%. The sender's pressure level and maximum/minimum angle information can also be included to filter out a few neighboring nodes that are not in the forwarding set. Furthermore, noting that there could be many other packets that must travel through a certain node and that the topology slowly changes over time, the set information may only need to be included in the data packet whenever there is a sufficient change. Thus, the amortized overhead could be much smaller.

V. RECOVERY MODE

A local lower-depth-first recovery method that guarantees the delivery is presented, and an efficient recovery route discovery method is provided using 2-D surface flooding, instead of the expensive 3-D flooding. Note that the opportunistic forwarding over a recovery path is illustrated in the extended version of this paper [46].

A. Local Lower-Depth-First Recovery

Unlike traditional geographic routing where the local minimum is determined using the location of a destination node, in the scenario in this paper, each node can easily determine whether it is on the local minimum by checking its neighbors; that is, a node is on the local minimum if there is no neighboring node with a lower pressure level. Therefore, a lower depth-first
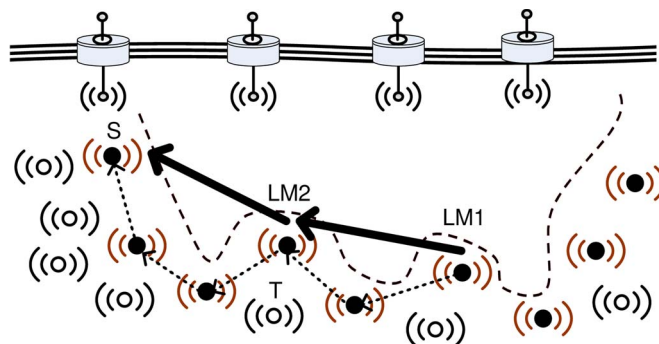

Fig. 4. Recovery mode.

recovery method is proposed as follows. Every local minimum node searches for a node whose depth is lower than its current depth, and they explicitly maintain a path to the node (via a route discovery method). This node could be another local minimum where there is a new recovery path or the point where the greedy forwarding can be resumed. Whenever a packet hits a local minimum, it is rerouted along the recovery path either safely to a node that can resume greedy forwarding or to a new local minimum. In Fig. 4, for example, there are two local minima, namely, $LM1$ and $LM2$. $LM1$ maintains a path to $LM2$, which has a path to node S. A packet can be routed from $LM1$ to $LM2$ to S. Then, it can be switched back to the greedy mode and can be delivered to a node on the ocean surface. In practice, the local minimum can be recovered after a few iterations.

The following theorem proves the delivery guarantee and loop-free property of the lower-depth-first routing.

Theorem 1: Local lower-depth-first routing is loop free and guarantees packet delivery.

Proof: Consider a local minimum graph $G = (V, E)$. A vertex $v \in V$ in the graph represents a local minimum node, and two vertices are connected if there is a recovery path. There is also a sink vertex that can reach the surface. If each vertex (local minimum) can reach the surface directly without visiting another local minima, it is connected to the sink. Assume that a packet arrives at a local minimum, e.g., vertex v_i. If v_i is connected to the sink, the packet is safely delivered. Otherwise, it will be rerouted to another local minimum (e.g., v_j) whose depth is lower than the current depth by definition, i.e., $D(v_i) > D(v_j)$, where $D(v_k)$ returns the depth of node v_k. Because the distance to the surface decreases in each step, a packet can be delivered after a finite number of steps that is strictly less than the total number of the local minima. This monotonic behavior also guarantees that there is no loop. ∎

B. 2-D Void Floor Surface Flooding for Recovery Path Search

Now, the important step is to determine the recovery route. The brute-force approach is 3-D flooding, that is, nodes at the local minima perform *expensive* hop-limited 3-D flooding to discover the escape nodes where the greedy mode can resume or to locate recovery paths to better escape nodes. This brute-force approach is not deemed suitable because the appropriate *scope* of the limited 3-D flooding is difficult to estimate, and the
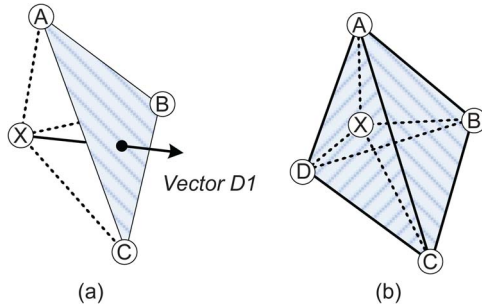
Fig. 5. Domination and nonsurface node. (a) Vector $D1$ is dominated. (b) Node X is not a surface node.

3-D flooding can degenerate to the network-wide flooding that involves all nodes in a sensor mesh. To improve efficiency, *2-D flooding on the void floor surface* is used. This flood involves a significantly more manageable set of nodes. Fig. 4 shows the approach in a 2-D network. Nodes on the envelope (or surface) become aware of their void floor surface status using local connectivity information and thus forward the packet. Nodes that are dominated by surface neighbors are not on the surface and refrain from forwarding. For example, node S does not have any nodes on its right and is a surface node. Node T is surrounded by its neighboring nodes, and it is not on the surface. Now, *domination* and a *void surface node* are formally defined for 3-D environments.

Definition 1: For a given node, a random vector emanating from the node is dominated if and only if there is a dominating triangle formed by the node's neighbors that intersects with the vector. A node is on the surface if and only if there exists a vector that is not dominated (i.e., no dominating triangle for the vector).

Consider Fig. 5(a). The random vector $D1$ emanating from node X is dominated because it intersects with the triangle ABC. Any random vector pointing inside the tetrahedron $XABC$ is dominated by the triangle. In Fig. 5(b), node X is completely surrounded by a set of tetrahedra that dominates every possible direction. Thus, node X is a nonsurface node. Surface node detection can be formally described as follows. Consider the point set P in 3-D Euclidean space where the set is composed of node X and its neighbors. Any pair of points in the set is connected if their distance is less than or equal to the transmission range. The point set centered at node X is now normalized (as a unit vector); thus, it is on the surface of a unit ball. The connectivity among the points in the normalized point set does not change. Given that we have a normalized point set and connectivity information among the set members, the surface node detection is undertaken to decompose the point set into a set of nonoverlapping tetrahedra that exhaustively cover the unit ball. It is known that the length constraints (due to the communication range) cause these types of tetrahedralization problems to be intractable [57], [58]. If a length constraint does not exist, the problem becomes a decomposition of the convex hull of P into nonoverlapping tetrahedra, which can be solved in $O(n \log n)$, where n is the point set size [59].

In this paper, a simple Monte Carlo approximation method is proposed: pick m random directions and check whether there is a dominating triangle for each direction. The number of directions, i.e., m, should be sufficiently large to correctly identify the surface node. Otherwise, the void floor surface detection may fail, which generates a false negative: A surface node is declared as a nonsurface node. The approximation method is detailed as follows. First, generate a set R of m random vectors. There are $O(n^3)$ triangles that can be formed by node X's neighbors. For each triangle, repeat the following procedure: check all vectors in the set R to determine whether they are dominated by the triangle or not and remove the dominated vectors from the set R. If R becomes empty, it is declared that node X is not on the void floor surface; otherwise, the algorithm declares that node X is on the void floor surface. Thus, the worst-case complexity is given as $\Theta(mn^3)$. Note that the detection algorithm is localized and requires only a one-hop topology, which can be constructed using only periodic beacons. Thus, it does not cause any additional packet exchanges. Moreover, the processing overhead is minimal because it is only triggered when nodes detect that the local network topology has sufficiently changed.

The accuracy of this method can be analyzed as follows. Let X be a node that is on the void floor surface. The volume of a sphere centered at node X is given by $(4/3)\pi R^3$, where R is the transmission range. Assuming that the volume of a void area that intersects with the sphere is x, a random vector hits the void area with a probability of $p = (3x/4\pi R^3)$. A false negative occurs when all m random vectors miss the void. Thus, the probability of a false negative is given as $(1 - p)^m$, which exponentially decreases with m. In practice, the volume size of a void is sufficiently large, and high accuracy can be achieved with a small m. For example, when the intersecting void volume is one fifth of the sphere ($p = 1/5$) and $m = 20$, the probability of a false negative is approximately 1%.

Thus far, it has been assumed that a void area always causes the local minimum. In the proposed pressure routing, not every void area causes the local minimum. Such void areas are usually located inside the swarm (á la the air bubbles in bread dough), and greedy forwarding can successfully bypass the void areas. This type of void is termed a *bubble*. The bubble size is closely related to the node density: As the node density increases, there will be fewer bubbles whose sizes are also diminishing. Fig. 5(b) shows that at least four nodes are required in order not to exclude a surface node. Given that a well-connected 3-D network requires each node to have approximately 30 neighbors (15 neighbors in 2-D networks) [47], these bubbles are likely to occur particularly when the node density is very low. In practice, the nodes on the bubble surface will not cause a problem. The special case that requires attention occurs when a bubble *contacts* the real void floor surface. Under this circumstance, those nodes will receive route discovery packets and also participate in the flooding process, which will cause redundant packet transmissions. To prevent this, nodes should be able to determine whether the void area is a bubble or not. However, this is an expensive process and requires more than two-hop information. This issue remains as future work for investigating how to efficiently manage this situation.

VI. SIMULATIONS

Here, the proposed approaches are evaluated via simulations using QualNet. First, the forwarding set selection is investigated to answer: How important is the hidden-terminal problem? How good are the proposed forwarding set selection heuristics? Second, the recovery mode is evaluated to answer: How often is a packet trapped in a local minimum for varying node density? How effective is the proposed void surface detection scheme? Finally, the performance of various depth-based routing strategies (e.g., different forward set selection methods and recovery modes) are compared.

A. Simulation Setup

For acoustic communications, the channel model in Section IV-A was implemented in the physical layer of Qual-Net. Different channel fading conditions were generated in the simulations by adjusting the transmission power in dB re μPa.[3] We use the underwater acoustic channel models described in [6] and [50] to estimate delivery probability. The path loss over a distance d for a signal of frequency f due to large-scale fading is given as $A(d, f) = d^k a(f)^d$, where k is the spreading factor, and $a(f)$ is the absorption coefficient. The geometry of propagation is described using the spreading factor ($1 \leq k \leq 2$); for a practical scenario, k is given as 1.5. The absorption coefficient $a(f)$ is described by Thorp's formula [50]. The average SNR over distance d is thus given as

$$\Gamma(d) = \frac{E_b/A(d, f)}{N_0} = \frac{E_b}{N_0 d^k a(f)^d} . x \qquad (8)$$

Here, E_b and N_0 are constants that represent the average transmission energy per bit and noise power density in a non-fading AWGN channel. As in [6] and [51], we use Rayleigh fading to model small-scale fading where the SNR has the following probability distribution:

$$p_d(X) = \frac{1}{\Gamma(d)} e^{-\frac{X}{\Gamma(d)}}. \qquad (9)$$

The probability of error can be evaluated as

$$p_e(d) = \int_0^\infty p_e(X) p_d(X) \, dX \qquad (10)$$

where $p_e(X)$ is the probability of error for an arbitrary modulation at a specific value of SNR X. In this paper, we use BPSK modulation because BPSK is widely used in the state-of-the-art acoustic modems [52]. In BPSK, each symbol carries a bit. In [53], the probability of bit error over distance d is given as

$$p_e(d) = \frac{1}{2} \left(1 - \sqrt{\frac{\Gamma(d)}{1 + \Gamma(d)}} \right). \qquad (11)$$

Thus, for any pair of nodes with distance d, the delivery probability of a packet with size m bits is simply given as

$$p(d, m) = (1 - p_e(d))^m. \qquad (12)$$

[3]The signal intensity is measured in decibels re μPa of the power flux $[W m^{-2}]$ delivered to the water by a source.

Unless otherwise stated, the transmission power is 105 dB re μPa. A transmission range of 250 m was used, and the data rate was set to be 50 Kb/s, as in [60]. The carrier-sense multiple access (CSMA) medium access control (MAC) protocol was also used. In CSMA, when the channel is busy, a node waits for a backoff period and senses the carrier again. Every packet transmission is MAC-layer broadcasting. For reliability, ARQ was implemented at the routing layer as follows. After packet reception, the receiver sends back a short ACK packet. If the sender fails to hear an ACK packet, a data packet is retransmitted, and the packet will be dropped after five retransmissions.

To evaluate the proposed protocol's behaviors with a passive mobility for underwater sensor nodes (i.e., Drogues), an extended 3-D version of the MCM model [16] was adopted to pattern the motility of each sensor node. Unlike most existing sensor node mobility patterns from the literature that assume that each node moves independently of all others and wherein its path vector is determined using an independent realization of a stochastic process, the MCM model considers fluid dynamics, whereby the same velocity field affects all nodes. Here, the MCM model considers the effect of the meandering subsurface currents (or jet streams) and vortices on the deployed nodes to pattern its path vector. In the simulations, varying numbers of nodes ranging from 100 to 450 were randomly deployed in the 3-D region of a size of 1000 m × 1000 m × 1000 m. The nodes were set to move with a maximum speed of 0.3 m/s. The average node densities for 150, 200, 250, 300, 350, 400, and 450 were given as 9, 12, 15, 18, 22, 25, and 28, respectively.

Each node measured the distance to its neighbors every 30 s (with random jitters to prevent synchronization) and broadcasted the measured information to its one-hop neighbors. Every 60 s, each node reported the sensed data and distance measurements to the surface. Note that a node in the main jet stream will have moved 20 m in 60 s. With a range of 250 m, it was expected that the 60-s refresh rate would be adequate to track topology changes for off-site localization. The packet size is a function of the number of neighbors, and the average packet size was less than 200 B in these simulations. The delivery ratio, delay, and overhead were also measured. The delivery ratio of a source is the fraction of the packets delivered, the delay is the time for a packet to reach any sink node on the surface, and the overhead was measured in terms of the total number of packet transmissions. In these simulations, each run lasted 3600 s. Unless otherwise specified, the average value of 50 runs with the 95% confidence interval is reported.

B. Simulation Results

In Section IV, it is demonstrated that the forwarding set selection and its prioritization must be appropriately undertaken to mitigate the hidden-terminal problem. Otherwise, there will be redundant transmissions and collisions. To illustrate the impact, a simple forwarding set selection method proposed in DBR [10] was evaluated. Recall that DBR is the first underwater routing scheme to exploit pressure (and, thus, depth) awareness at each node for routing packets to the surface. It implements a basic greedy forwarding design with an opportunistic forwarding manner. All nodes higher than the current
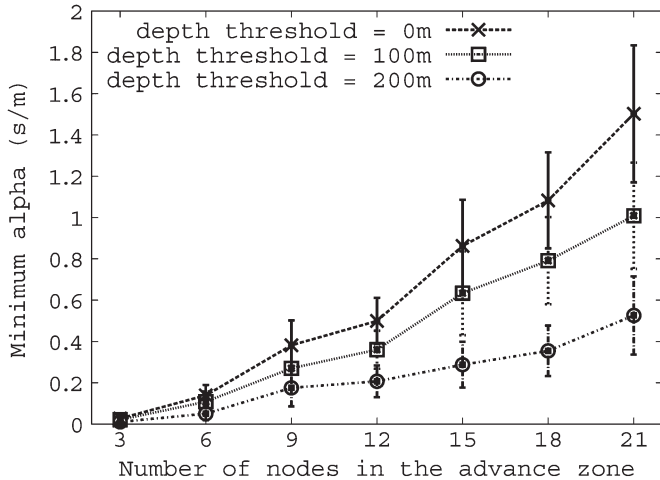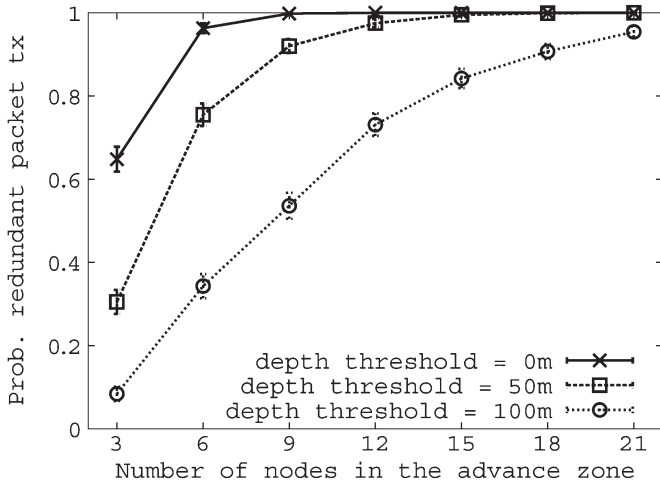
Fig. 6.   Minimum alpha value.

Fig. 8.   EPAs of different forwarding set selection schemes.

Fig. 7.   Probability of a redundant packet transmission.

forwarder by more than a depth threshold (h) function as opportunistic forwarders. Moreover, nodes use a fixed α value for timer setting. However, we show that α values should be carefully set on the basis of a network topology. We randomly deploy varying numbers of nodes in the hemisphere (three to 21 nodes). For a given number of nodes, we generate 1000 random topologies. For each configuration, we calculate the minimum α value using (7) using three different minimum depth thresholds ($h = 0$, 100, 200 m). We plot the average α value of 1000 random topologies with 95% confidence interval. Fig. 6 clearly shows that as density increases, it is more likely that two nodes are in close proximity (or have low depth difference), and thus, the average minimum alpha value significantly increases. For example, the alpha value of one can result in the maximum delay of 250 s in our scenario. In Fig. 7, we plot the probability of redundant packet transmissions caused by the hidden-terminal problem, i.e., if there are multiple forwarders that are hidden from one another, those nodes will transmit packets redundantly. We calculated the probability by dividing the number of instances having a redundant packet transmission by the total number of random topologies (i.e., 1000). The graph shows that the larger the number of nodes in the advance zone, the higher the probability of redundant packet transmis-
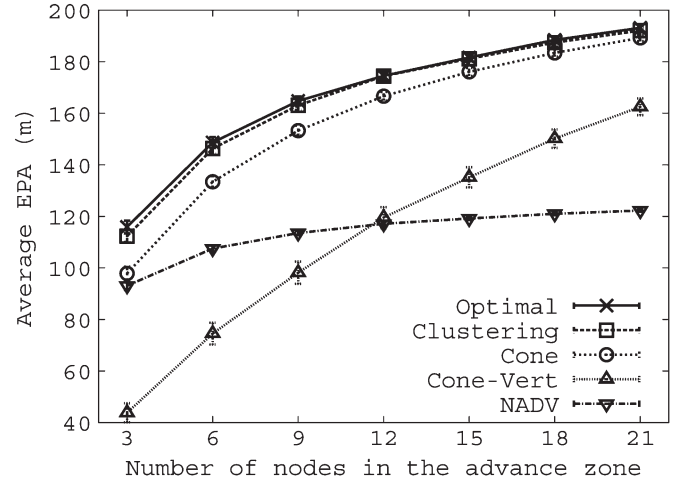
sions. If we have higher depth threshold, there will be a smaller number of candidate forwarding nodes, and the probability of redundant packet transmissions will be lower. The results clearly show that the hidden-terminal problem persists even with a high depth difference value. For instance, a ten-node scenario has more than a 60% chance of redundant packet transmissions with depth difference of 100 m. Therefore, it is mandatory to suppress such redundant transmissions.

Now, the effectiveness of the proposed forwarding set selection algorithm is evaluated. In Fig. 8, the progress (EPA) of the different forwarding set selection schemes (optimal, cone-based, clustering, and simple NADV) is plotted. In the optimal scheme, an exhaustive search was performed on the neighbor set to determine the maximum EPA. NADV denotes the case where only the node whose NADV was the largest was chosen (i.e., a single node in the forwarding set). Cone-Vert only considered the vertical direction as in [13] and [14] (see Table I for the terminology and its definition). The figure demonstrates that the proposed clustering method was very close to the optimal solution and that it outperformed the cone-based approaches. The results also demonstrate that the greater the number of nodes, the higher the EPA (as expected).

The fraction of local minimum nodes over time under MCM mobility (half a day) was also measured. Because this is closely related to node density, the number of nodes was varied ranging from 100 to 400. For a given configuration, the number of local minimum nodes was sampled every 1.7 h. Fig. 9 presents the results. When the node density was low, the fraction of the local minimum nodes was high. As time passed, the fraction of the local minimum nodes increased. This resulted from the nodes tending to disperse over the simulated area (beyond the original $1000 \times 1000 \times 1000$ cube) due to the ocean currents (i.e., jet streams and vortices).

The accuracy of the proposed void floor surface detection method was also analyzed. The fraction of the surface nodes detected was measured by varying the number of nodes in the network (100–400) and the number of random vectors ($k = 1 - 1000$). For clarity, the number of detected surface nodes was divided by that for $k = 10\,000$. Fig. 10 presents the results. The lower the density, the higher the detection probability

TABLE I
TERMINOLOGY

| Terms	Definitions
EPA	Expected Packet Advance toward destination
$NADV$	A forwarding set selection based on Normalized Advance
$Cone$	A forwarding set selection that considers nodes in the cone shape
$Cone\text{-}Vert$	A forwarding set selection that considers nodes in the vertical direction cone shap
$SD\text{-}R$	A recovery scheme that uses 2D surface flooding
$SD\text{-}A$	A recovery scheme that uses angle-based selection heuristic (< 60 degrees)
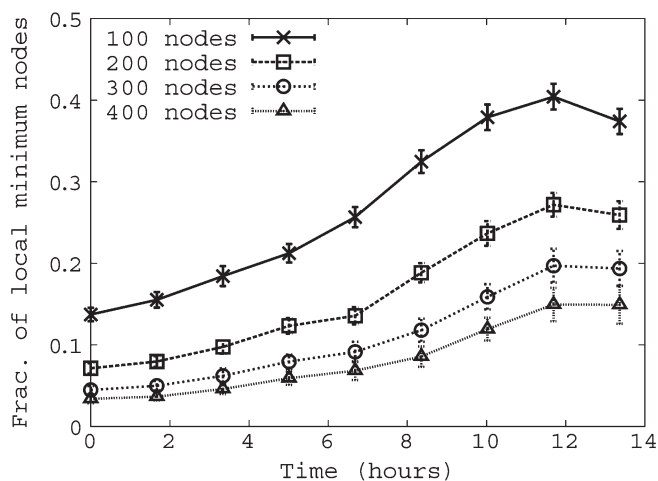
Fig. 9. Fraction of local minimum nodes over time.
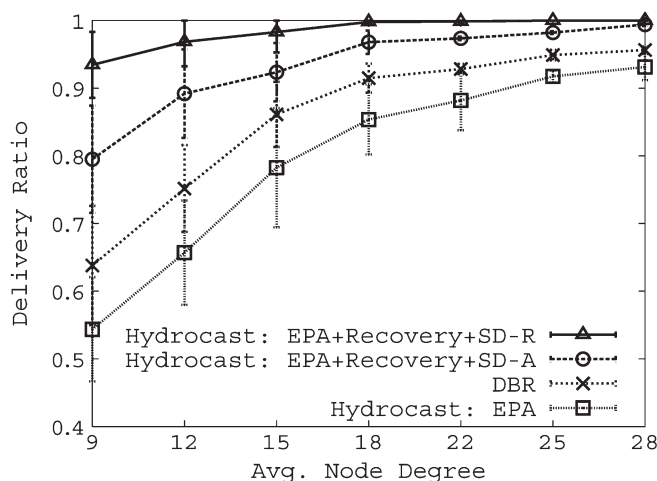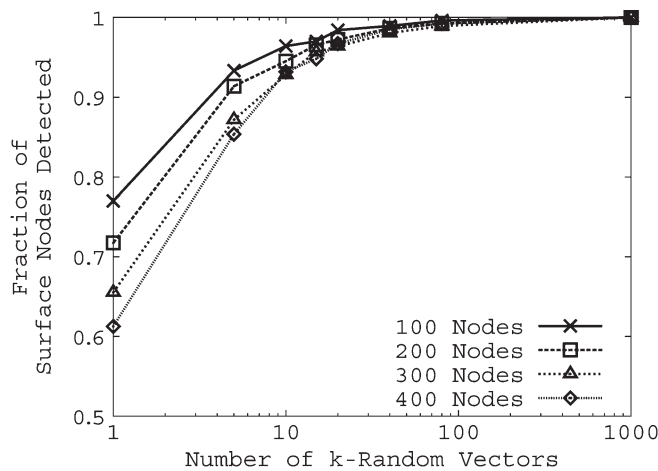

Fig. 11. Packet delivery ratio.

Fig. 10. Void floor surface detection using a Monte Carlo method.

because the area that intersects the void was larger (i.e., a larger p). As the number of random vectors increased, the detection probability approached 1. The figure shows that the detection probability was more than 95% with $k = 20$.

Finally, the performance of HydroCast was compared with DBR under different settings. Recall that DBR implements a basic greedy forwarding design with opportunistic forwarding and uses a fixed holding timer at each hop. HydroCast uses a more elaborate opportunistic forwarding strategy and supports recovery from voids. To demonstrate the benefit of the proposed 2-D surface flooding (denoted as SD-R), a simple angle-based selection heuristic was also implemented, i.e., when a node X broadcasted a route discovery packet, any neighboring node

A whose adjacent angle formed by the X-axis and XA was less than $60°$ participated in the flooding (denoted as SD-A). See Table I for the terminology and its definition. Fig. 11 presents the packet delivery ratio. When the node density was low, DBR had a higher delivery ratio than HydroCast without recovery. Unlike HydroCast, DBR did not suppress redundant packet transmissions; thus, it delivered packets on multiple paths, which improved the reliability. The same figure also presents the plot for HydroCast with forwarding set selection and recovery. It should be noted that the recovery support from the voids significantly improved the reliability of HydroCast and put it above DBR. The accurate surface detection assisted in achieving better PDR because the angle-based selection might not include some surface nodes, which then fail to locate the recovery path (particularly when the density is low).

In Fig. 12, the average number of packet transmissions to deliver a data packet is plotted including the recovery process. Due to the redundant packet transmissions and multipath packet delivery, the DBR resulted in significantly more transmissions than the other schemes. Interestingly, the impact of recovery was reduced as the density increased because there were fewer voids and fewer hops to switch back to the greedy mode, and more nodes were involved in packet forwarding; thus, the amortized recovery cost decreased. For the angle-based selection, the overall overhead remained the same because there were more redundant packet transmissions as the density increased (fewer voids, but much higher costs). Finally, Fig. 13 shows that HydroCast had a lower end-to-end delay than DBR due to its adaptive timer setting at each hop. As the density decreased,
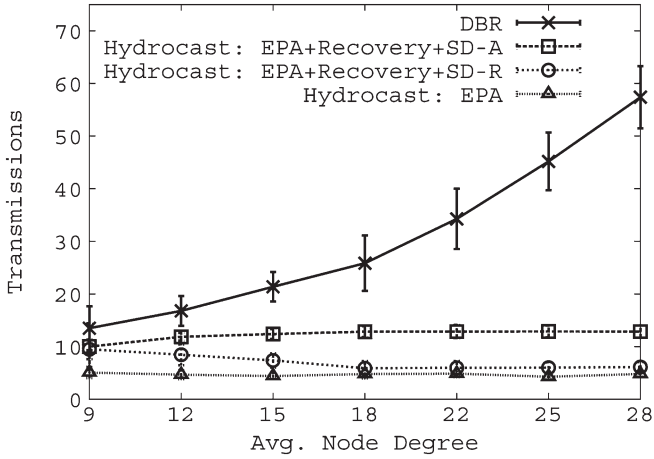
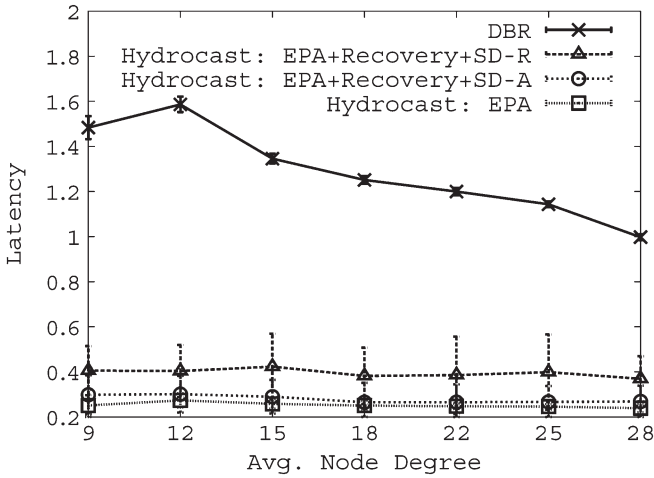Fig. 12.   Number of transmissions for delivery.

Fig. 13.   Average end-to-end delay.

the average delay in HydroCast slightly increased as a result of the increased frequency of voids requiring recovery and, thus, longer paths.

C. AUV Dynamics

To explore and observe the ocean with a wider area coverage in an active manner, a swarm of AUVs such as REMUS and IVER2 can be deployed to the venue of interest. To evaluate the performance with the relatively high speed underwater mobility of AUVs, a well-known AUV mobility model that considers AUV dynamics underwater was used [17]. Regarding the vehicle dynamics, most AUVs fall into the category of underactuated vehicles for which the number of actuators is smaller than its degrees of freedom in motion. That is, a typical AUV (or underwater vehicle) moving in 3-D space has six degrees of freedom (i.e., surge, sway, heave, roll, pitch, and yaw) in an active manner; however, the vehicle's control configuration with conventional thrusters and fins allows for limited motions in space. For example, in general, AUVs cannot freely move in the lateral direction. To describe the motion of AUVs considering this type of motion constraint, the kinematic point-mass vehicle model is introduced [17]. The equations of

motion for an individual vehicle can be expressed in the state-variable form as follows:

$$
\begin{bmatrix} \dot{x} \\ \dot{y} \\ \dot{z} \\ \dot{\chi} \\ \dot{\gamma} \\ \dot{V} \end{bmatrix} = \begin{bmatrix} V \cos \gamma \cos \chi \\ V \cos \gamma \sin \chi \\ V \sin \gamma \\ r \\ q \\ a \end{bmatrix} + \mathbf{w} \tag{13}
$$

where x is the x-position, y is the y-position, z is the z-position, V is the longitudinal speed, γ is the flight angle, and χ is the heading angle. Furthermore, r, q, and a are the control inputs that represent the heading angle rate, flight angle rate, and longitudinal acceleration, respectively. $\mathbf{w}$ is the process noise due to environmental disturbances such as ocean currents and waves.

In this paper, operation scenarios involving multiple AUVs are considered. For convenience, it is assumed that the AUVSs are separated by altitude for collision avoidance and that they are cruising at a constant speed. Then, a simpler expression for the equations of motion can be obtained by setting the flight angle γ and the longitudinal acceleration a to zero, shown as follows:

$$
\begin{bmatrix} \dot{x} \\ \dot{y} \\ \dot{\chi} \end{bmatrix} = \begin{bmatrix} V \cos \chi \\ V \sin \chi \\ r \end{bmatrix} + \mathbf{w} \tag{14}
$$

with $\dot{z} = \dot{V} = 0$.

A set of time trajectories was calculated using the vehicle model described above. For this, a sequence of waypoints was assigned for each vehicle, and the vehicles were controlled to track them. The waypoint tracking control was conducted using the line-of-sight (LOS) guidance law [17], i.e.,

$$
r = k_p \phi + k_d \dot{\phi} \tag{15}
$$

where ϕ is the LOS angle to the next waypoint, and $\dot{\phi}$ is the LOS rate. k_p and k_d are the control gains for the proportional derivative controller employed here. Note that ϕ and $\dot{\phi}$ are functions of the vehicle's motion and waypoint configuration.

To evaluate the proposed protocol's behaviors under dynamic AUV mobility, varying numbers of AUVs ranging from 20 to 100 were randomly deployed in a 3-D region with a size of 5 km × 5 km × 5 km. A transmission range of 1000 m was used, and the maximum speed of the AUVs was varied from 1 knot (0.514 m/s) to 15 knots (7.716 m/s). Each AUV reported the sensed data and distance measurements to the surface at 60-s intervals. The packet size is a function of the number of neighbors, and the average packet size was less than 200 B in these simulations. The delivery ratio and energy consumption were also measured. Note that the delivery ratio of a source is the fraction of packets delivered. In these simulations, each run lasts 3600 s.

The performances of different types of HydroCast (i.e., without recovery, SD-R, and SD-A) were compared with DBR under dynamic AUV mobility. Fig. 14 presents the packet delivery ratio when the maximum speed of an AUV was 1 knot (independent but slow mobility). This figure shows similar behaviors to those in Fig. 11. In a low AUV density, DBR had a higher delivery ratio than HydroCast without recovery
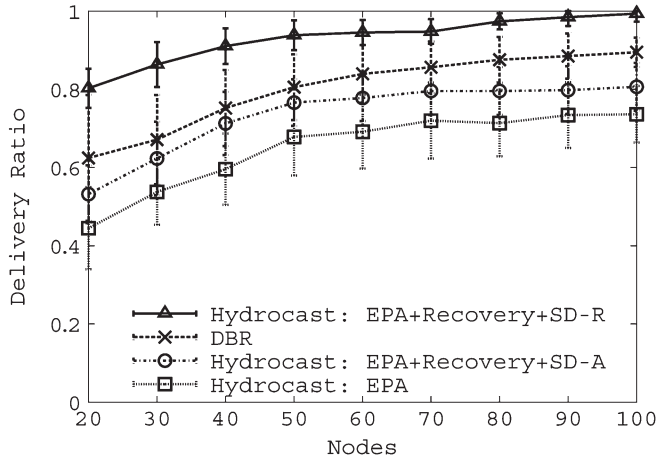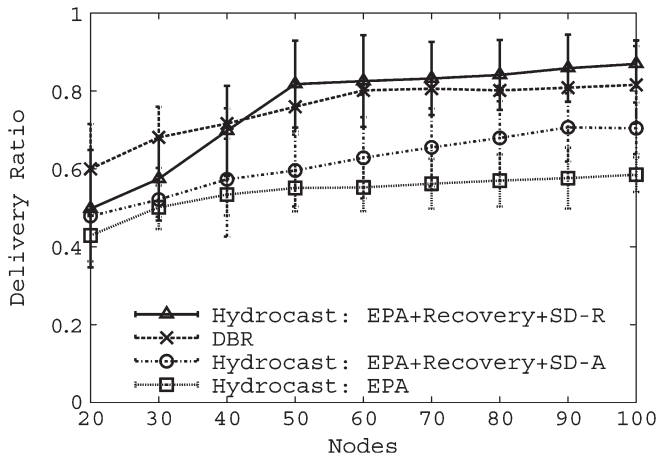
Fig. 14. PDR: 1 knot.

Fig. 15. PDR: 15 knots.

and SD-A because DBR delivered packets using multiple paths as a result of the redundant packet transmissions. However, the HydroCast with forwarding set selection and recovery (i.e., SD-R) significantly improved its reliability and surpassed the delivery ratio of DBR. It is noteworthy that all four protocols experienced degraded PDR performance because they cannot exploit the passive group mobility. This performance degradation was severe in HydroCast without recovery and SD-A. The SD-A's angle-based selection was not robust to the AUV's independent mobility, and it exhibited a lower delivery ratio than that of DBR. Unlike SD-A, SD-R outperformed DBR. Fig. 15 presents the packet delivery ratio when the maximum speed of the AUV was 15 knots (independent and fast mobility). Due to the high speed mobility, all three HydroCast types exhibited a degraded delivery ratio performance. This effect was unavoidable for SD-R, particularly when the AUV density was low. This results from the fact that some of SD-R's recovery paths were broken due to the high mobility. Unlike the HydroCast protocols, DBR exhibited robustness to the fast and independent mobility because the DBR did not suppressed redundant transmissions and primarily relied on the multipath delivery. However, HydroCast can be extended to achieve similar levels of robustness against the fast and independent mobility scenarios if we selectively maintain multipath routes
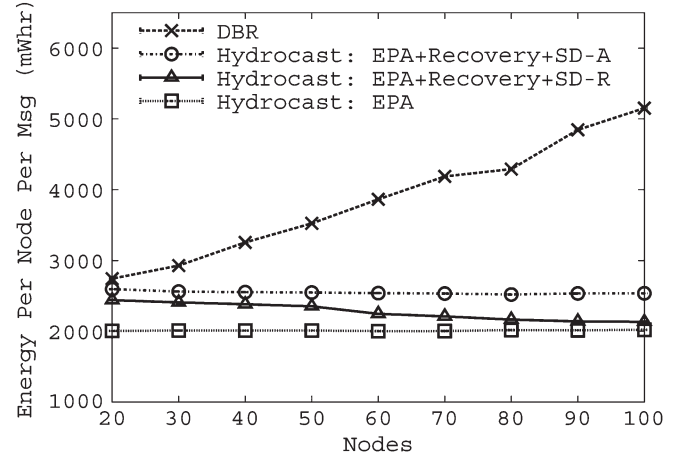

Fig. 16. Average end-to-end energy consumption.

(i.e., relaxed redundant packet suppression). This extension is part of our future work.

In Fig. 16, the average energy consumption of the delivered data packets from Fig. 15 is plotted. The DBR exhibited a robust delivery ratio performance to fast and independent mobility as a result of its multipath packet delivery at the expense of redundant packet transmissions. Thus, the DBR consumed significantly more energy for each packet delivery than the other schemes (even worse with a high AUV density). Due to the absence of recovery, the HydroCast without recovery exhibited the minimum energy consumption. In SD-R, the recovery cost reduced as the density increased. This resulted from there being fewer opportunities to confront voids and thus resulting in recovery cost decreases. In SD-A, the overall overhead remained the same due to the angle-based recovery nature. As the density increased, the opportunity to confront voids was reduced, but the cost of the angle-based recovery increased.

VII. CONCLUSION

Hydraulic-pressure-based anycast routing that allows time-critical sensor data to be reported to sonobuoys at sea level using acoustic multihopping has been investigated. Because acoustic transmissions are power hungry, the research goal was to minimize the number of packet transmissions in underwater sensor deployments that are challenged by ocean currents, unreliable acoustic channels, and voids. In this paper, the HydroCast method was proposed: It is a hydraulic-pressure-based anycast routing protocol with salient features of novel opportunistic routing mechanisms to select the subset of forwarders that maximizes the greedy progress yet limits the cochannel interference. It is also an efficient underwater *dead end* recovery method that outperforms the recently proposed approaches (e.g., random walk, 3-D flooding, etc.). The simulation results confirmed that the proposed protocols could effectively manage the challenges.

REFERENCES

[1] I. F. Akyildiz, D. Pompili, and T. Melodia, "Underwater acoustic sensor networks: Research challenges," *Ad Hoc Netw.*, vol. 3, no. 3, pp. 257–279, Mar. 2005.

[2] J. Kong, J.-H. Cui, D. Wu, and M. Gerla, "Building underwater ad-hoc networks and sensor networks for large scale real-time aquatic applications," in *Proc. IEEE MILCOM*, Oct. 2005, pp. 1535–1541.

[3] U. Lee, J. Kong, J.-S. Park, E. Magistretti, and M. Gerla, "Time-critical underwater sensor diffusion with no proactive exchanges and negligible reactive floods," in *Proc. IEEE ISCC*, Jun. 2006, pp. 609–615.

[4] Z. Zhou, J.-H. Cui, and A. Bagtzoglou, "Scalable localization with mobility prediction for underwater sensor networks," in *Proc. IEEE INFOCOM*, Apr. 2008, pp. 211–215.

[5] J. Jaffe and C. Schurgers, "Sensor networks of freely drifting autonomous underwater explorers," in *Proc. WUWNet*, Sep. 2006, pp. 93–96.

[6] M. Stojanovic, "On the relationship between capacity and distance in an underwater acoustic communication channel," in *Proc. WUWNet*, Sep. 2006, pp. 41–47.

[7] S. Durocher, D. Kirkpatrick, and L. Narayanan, "On routing with guaranteed delivery in three-dimensional ad hoc wireless networks," in *Proc. ICDCN*, Jan. 2008, pp. 227–235.

[8] R. Flury and R. Wattenhofer, "Randomized 3D geographic routing," in *Proc. IEEE INFOCOM*, Apr. 2008, pp. 1508–1516.

[9] B. Jalving, "Depth accuracy in seabed mapping with underwater vehicles," in *Proc. MTS/IEEE OCEANS Riding Crest 21st Century*, Sep. 1999, pp. 973–978.

[10] H. Yan, Z. Shi, and J.-H. Cui, "DBR: Depth-based routing for underwater sensor networks," in *Proc. IFIP Netw.*, May 2008, pp. 72–86.

[11] B. Karp and H. T. Kung, "GPSR: Greedy perimeter stateless routing for wireless networks," in *Proc. MobiCom*, Aug. 2000, pp. 243–254.

[12] V. Chandrasekhar, Y. S. Choo, and H. V. Ee, "Localization in underwater sensor networks—Survey and challenges," in *Proc. WUWNet*, Sep. 2006, pp. 33–40.

[13] H. Füßler, J. Widmer, M. Käsemann, M. Mauve, and H. Hartenstein, "Contention-based forwarding for mobile ad-hoc networks," *Ad Hoc Netw.*, vol. 1, no. 4, pp. 351–369, Nov. 2003.

[14] M. Zorzi and R. R. Rao, "Geographic Random Forwarding (GeRaF) for ad hoc and sensor networks: Energy and latency performance," *IEEE Trans. Mobile Comput.*, vol. 2, no. 4, pp. 349–365, Oct.–Dec. 2003.

[15] J. M. Jornet, M. Stojanovic, and M. Zorzi, "Focused beam routing protocol for underwater acoustic networks," in *Proc. WUWNet*, Sep. 2008, pp. 75–82.

[16] A. Caruso, F. Paparella, L. F. M. Vieira, M. Erol, and M. Gerla, "The meandering current model and its application to underwater sensor networks," in *Proc. IEEE INFOCOM*, Apr. 2008, pp. 771–779.

[17] T. I. Fossen, *Guidance and Control of Ocean Vehicles*. Hoboken, NJ, USA: Wiley, 1994.

[18] J. Bellingham, *Autonomous Underwater Vehicles (AUVs)*. San Diego, CA, USA: Academic, 2001.

[19] S. Roy, P. Arabshahi, D. Rouseff, and W. Fox, "Wide area ocean networks: Architecture and system design considerations," in *Proc. WUWNet*, Sep. 2006, pp. 25–32.

[20] W. J. Gould and W. J. Gould, "Argo-sounding the oceans," *Weather*, vol. 61, no. 1, pp. 17–21, Jan. 2006.

[21] D. Kilfoyle and A. Baggeroer, "The state of the art in underwater acoustic telemetry," *IEEE J. Ocean. Eng.*, vol. 25, no. 1, pp. 4–27, Jan. 2000.

[22] F. M. Yaul, "A flexible underwater pressure sensor array for artificial lateral line applications," M.S. thesis, Dept. Elect. Eng. Comput. Sci., Cambridge, MA, USA, Mass. Inst. Technol., 2011.

[23] "BMP085: Digital, Barometric Pressure Sensor," BOSCH, Stuttgart, Germany, 2008, http://www.bosch-sensortec.com.

[24] K. Muralidharan, A. J. Khan, A. Misra, R. K. Balan, and S. Agarwal, "Barometric phone sensors: More hype than hope!," in *Proc. HotMobile*, 2014, pp. 12:1–12:6.

[25] E. Gallimore *et al.*, "The WHOI micromodem-2: A scalable system for acoustic communications and networking," in *Proc. OCEANS*, Sep. 2010, pp. 1–7.

[26] D. Pompili, T. Melodia, and I. F. Akyildiz, "Routing algorithms for delay-insensitive and delay-sensitive applications in underwater sensor networks," in *Proc. MobiCom*, Sep. 2006, pp. 298–309.

[27] P. Xie, J.-H. Cui, and L. Lao, "VBF: Vector-based forwarding protocol for underwater sensor networks," in *Proc. NETWORKING*, 2006, pp. 1216–1221.

[28] A. Savvides, C.-C. Han, and M. B. Strivastava, "Dynamic fine-grained localization in ad-hoc wireless sensor networks," in *Proc. MobiCom*, Jul. 2001, pp. 166–179.

[29] P. Biswas and Y. Ye, "Semidefinite programming for ad hoc wireless sensor network localization," in *Proc. IPSN*, Apr. 2004, pp. 46–54.

[30] M. Ayaz and A. Abdullah, "Hop-by-Hop Dynamic Addressing Based (H2-DAB) routing protocol for underwater wireless sensor networks," in *Proc. ICIMT*, 2009, pp. 436–441.

[31] P. Casari and A. F. Harris, "Energy-efficient reliable broadcast in underwater acoustic networks," in *Proc. WuWNet*, 2007, pp. 49–56.

[32] P. Casari, M. Rossi, and M. Zorzi, "Towards optimal broadcasting policies for HARQ based on fountain codes in underwater networks," in *Proc. WONS*, 2008, pp. 11–19.

[33] P. Nicopolitidis, G. Papadimitriou, and A. Pomportsis, "Adaptive data broadcasting in underwater wireless networks," *IEEE J. Ocean. Eng.*, vol. 35, no. 3, pp. 623–634, Jul. 2010.

[34] J. Xu, K. Li, and G. Min, "Reliable and energy-efficient multipath communications in underwater sensor networks," *IEEE Trans. Parallel Distrib. Syst.*, vol. 23, no. 7, pp. 1326–1335, Jul. 2012.

[35] P. Casari, A. Asterjadhi, and M. Zorzi, "On channel aware routing policies in shallow water acoustic networks," in *Proc. OCEANS*, 2011, pp. 1–6.

[36] C.-Y. Huang, P. Ramanathan, and K. Saluja, "Routing TCP flows in underwater mesh networks," *IEEE J. Sel. Areas Commun.*, vol. 29, no. 10, pp. 2022–2032, Dec. 2011.

[37] Y. Noh, U. Lee, P. Wang, B. S. C. Choi, and M. Gerla, "VAPR: Void-aware pressure routing for underwater sensor networks," *IEEE Trans. Mobile Comput.*, vol. 12, no. 5, pp. 895–908, May 2013.

[38] M. Ayaz, I. Baig, A. Azween, and F. Ibrahima, "A survey on routing techniques in underwater wireless sensor networks," *J. Netw. Comput. Appl.*, vol. 34, no. 6, pp. 1908–1927, Nov. 2011.

[39] S. Lee, B. Bhattacharjee, and S. Banerjee, "Efficient geographic routing in multihop wireless networks," in *Proc. MOBIHOC*, May 2005, pp. 230–241.

[40] S. Biswas and R. Morris, "Opportunistic routing in multi-hop wireless networks," in *Proc. SIGCOMM*, Aug. 2005, pp. 69–74.

[41] H. Dubois-Ferriere, M. Grossglauser, and M. Vetterli, "Least-cost opportunistic routing," in *Proc. Allerton*, Sep. 2007, pp. 1–8.

[42] K. Zeng, W. Lou, J. Yang, and D. R. Brown, "On geographic collaborative forwarding in wireless ad hoc and sensor networks," in *Proc. WASA*, Aug. 2007, pp. 11–18.

[43] B. Leong, B. Liskov, and R. Morris, "Geographic routing without planarization," in *Proc. NSDI*, May 2006, pp. 25:1–25:14.

[44] K. Liu and N. B. Abu-Ghazaleh, "Virtual coordinate backtracking for void traversal in geographic routing," in *Proc. ADHOC-NOW*, Aug. 2006, pp. 46–59.

[45] B. Zhou, Y. Z. Lee, M. Gerla, and F. de Rango, "Geo-LANMAR: A scalable routing protocol for ad hoc networks with group motion," *Wireless Commun. Mobile Comput.*, vol. 6, no. 7, pp. 989–1002, Nov. 2006.

[46] U. Lee *et al.*, "Pressure routing for underwater sensor networks," Univ. Calif. Los Angeles, Los Angeles, CA, USA, Tech. Rep., 2009.

[47] S. Poduri, S. Pattem, B. Krishnamachari, and G. S. Sukhatme, "Sensor network configuration and the curse of dimensionality," in *Proc. IEEE EmNets Workshops*, Cambridge, MA, USA, May 2006.

[48] M. O'Rourke, E. Basha, and C. Detweiler, "Multi-modal communications in underwater sensor networks using depth adjustment," in *Proc. WUWNet*, 2012, pp. 31:1–31:5.

[49] T. He, J. Stankovic, C. Lu, and T. Abdelzaher, "SPEED: A stateless protocol for real-time communication in sensor networks," in *Proc. ICDCS*, May 2003, pp. 46–55.

[50] L. M. Brekhovskikh and Y. Lysanov, *Fundamentals of Ocean Acoustics*, 3rd ed. New York, NY, USA: Springer-Verlag, 2003.

[51] C. Carbonelli and U. Mitra, "Cooperative multihop communication for underwater acoustic networks," in *Proc. WUWNet*, Sep. 2006, pp. 97–100.

[52] L. Freitag *et al.*, "The WHOI micro-modem: An acoustic communications and navigation system for multiple platforms," in *Proc. MTS/IEEE OCEANS*, Sep. 2005, pp. 1086–1092.

[53] T. Rappaport, *Wireless Communications: Principles and Practice*, 2nd ed. Boca Raton, FL, USA: CRC, 2002.

[54] P. Jacquet *et al.*, "Optimized link state routing protocol for ad hoc networks," in *Proc. IEEE INMIC*, 2001, pp. 62–68.

[55] D. Goldenberg *et al.*, "Localization in sparse networks using sweeps," in *Proc. MOBICOM*, Sep. 2006, pp. 110–121.

[56] L. Fan, P. Cao, and J. Almeida, "Summary cache: A scalable wide-area web cache sharing protocol," in *Proc. SIGCOMM*, Aug./Sep. 1998, pp. 254–265.

[57] J. Ruppert and R. Seidel, "On the difficulty of tetrahedralizing 3-dimensional non-convex polyhedra," in *Proc. ACM Symp. Comput. Geometry*, Jun. 1989, pp. 380–392.

[58] S. P. Y. Fung, C.-A. Wang, and F. Y. L. Chin, "*Approximation Algorithms for Some Optimal 2D and 3D Triangulations*," ser. Handbook of Approximation Algorithms and Metaheuristics, vol. 50. Upper Saddle River, NJ, USA: Prentice-Hall, 2007.

[59] H. Edelsbrunner, F. P. Preparata, and D. B. West, "Tetrahedrizing point sets in three dimensions," *J. Symbol. Algebraic Comput.*, vol. 10, no. 3/4, pp. 335–347, Sep./Oct. 1990.

[60] Z. Zhou and J.-H. Cui, "Energy efficient multi-path communication for time-critical applications in underwater sensor networks," in *Proc. MobiHoc*, May 2008, pp. 221–230.

Youngtae Noh (M'13) received the B.S. degree in computer science from Chosun University, Gwangju, Korea, in 2005; the M.S. degree in information and communication from Gwangju Institute of Science Technology, Gwangju, in 2007; and the Ph.D. degree in computer science from the University of California, Los Angeles, CA, USA, in 2012.

He is a Postdoctoral Research Associate with the Department of Computer Science, Purdue University, West Lafayette, IN, USA. His research areas include data center networking, wireless networking, future Internet, and mobile/pervasive computing.

Uichin Lee (M'13) received the B.S. degree in computer engineering from Chonbuk National University, Jeonju, Korea, in 2001; the M.S. degree in computer science from the Korea Advanced Institute of Science and Technology (KAIST), Daejeon, Korea, in 2003; and the Ph.D. degree in computer science from the University of California, Los Angeles, CA, USA, in 2008.

He is an Assistant Professor with the Department of Knowledge Service Engineering, KAIST. Before joining KAIST, he was a Member of Technical Staff with Bell Laboratories, Alcatel-Lucent, until 2010. His research interests include distributed systems and mobile/pervasive computing.

Saewoom Lee (M'14) received the B.Eng. degree in information and communication from Sungkyunkwan University, Seoul, Korea, in 2005 and the M.Eng. degree in information and communication from the Gwangju Institute of Science and Technology, Gwangju, Korea, in 2007, where he is currently working toward the Ph.D. degree.

His current research interests include routing protocols, secure routing protocols, and sensor authentication in wireless and mobile communication networks.
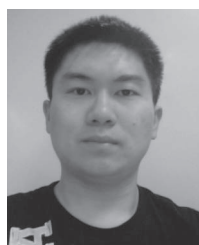
Paul Wang received the B.S. degree in computer science and economics from the University of California, San Diego, CA, USA, in 2006 and the M.S. degree in computer science from the University of California, Los Angeles, CA, USA, in 2010.

He is a Senior Software Engineer with Morgan Stanley & Co. LLC, New York, NY, USA. Prior to joining Morgan Stanley, he was a Software Engineer with Knight Capital Group, Inc., and a Systems Software Engineer with NASA's Jet Propulsion Laboratory, Pasadena, CA. His research interests include distributed systems, ad hoc and challenged networks, mobile computing, and large-scale database systems.

Luiz F. M. Vieira (M'10) received the B.S. and M.S. degrees from the Universidade Federal de Minas Gerais (UFMG), Belo Horizonte, Brazil, in 2002 and 2004, respectively, and the Ph.D. degree in computer science from the University of California, Los Angeles, CA, USA, in 2009.

Since 2010, he has been an Assistant Professor with the Department of Computer Science, UFMG. His research interest includes wireless, sensor, and underwater networks.

Dr. Vieira has received several awards, including the CNPq Research Fellowship.

Jun-Hong Cui (M'03) received the B.S. degree in computer science from Jilin University, Changchun, China, in 1995; the M.S. degree in computer engineering from the Chinese Academy of Sciences, Beijing, China, in 1998; and the Ph.D. degree in computer science from the University of California, Los Angeles, CA, USA, in 2003.

She is currently with the faculty of the Computer Science and Engineering Department, University of Connecticut, Storrs, CT, USA. Her research interests cover the design, modeling, and performance evaluation of networks and distributed systems. Recently, her research has mainly focused on exploiting the spatial properties in the modeling of network topology, network mobility, and group membership, scalable and efficient communication support in overlay and peer-to-peer networks, and algorithm and protocol design in underwater sensor networks.

Dr. Cui is actively involved in the community as an organizer, a Technical Program Committee Member, and a Reviewer for many conferences and journals. She has served as a Guest Editor for Elsevier's *Ad Hoc Networks* on two special issues (one on underwater networks and the other on wireless communication in challenged environments), and she now serves as an Associate Editor. She cofounded the first ACM International Workshop on UnderWater Networks (WUWNet 06), and she is now serving as the WUWNet Steering Committee Chair. She received the U.S. National Science Foundation CAREER Award in 2007 and the Office of Naval Research Yong Investigator Program Award in 2008. She is a member of the Association for Computing Machinery (ACM), ACM SIGCOMM, ACM SIGMOBILE, the IEEE Computer Society, and the IEEE Communications Society. (More information about her research can be found at http://www.cse.uconn.edu/jcui.)

Mario Gerla (F'02) received the degree in engineering from Politecnico di Milano, Milano, Italy, and the Ph.D. degree from the University of California, Los Angeles (UCLA), CA, USA.

From 1973 to 1976, he was with Network Analysis Corporation, New York, NY, USA, where he helped transfer ARPANET technology to government and commercial networks. In 1976, he joined UCLA, where he is currently a Professor of computer science. At UCLA, he was part of the team that developed the early ARPANET protocols under the guidance of Prof. L. Kleinrock. He has also designed and implemented network protocols, including ad hoc wireless clustering, multicast (ODMRP and CodeCast), and Internet transport (TCP Westwood). He has lead the $12M six-year ONR MINUTEMAN project, designing the next-generation scalable airborne Internet for tactical and homeland defense scenarios. He is currently leading two advanced wireless network projects under U.S. Army and IBM funding. His team is developing a vehicular testbed for safe navigation, urban sensing, and intelligent transport. A parallel research activity explores personal communications for cooperative networked medical monitoring (see www.cs.ucla.edu/NRL for recent publications).

Kiseon Kim (M'84–SM'98) received the B.Eng. and M.Eng. degrees in electronics engineering from Seoul National University, Seoul, Korea, in 1978 and 1980, respectively, and the Ph.D. degree in electrical engineering systems from the University of Southern California, Los Angeles, CA, USA, in 1987.

From 1988 to 1991, he was with Schlumberger, Houston, TX, USA. From 1991 to 1994, he was with the Superconducting Super Collider Lab, TX. In 1994, he joined Gwangju Institute of Science and Technology, Gwangju, Korea, where he is currently a Professor. His current interests include wideband digital communications system design, sensor network design, and analysis and implementation both at the physical layer and at the resource management layer.